ELSEVIER

Catalysis Today 28 (1996) 175–182

CATALYSIS TODAY

Photocatalytic water splitting on nickel intercalated $A_4Ta_xNb_{6-x}O_{17}$ (A = K, Rb)

K. Sayama [a,*], H. Arakawa [a], K. Domen [b]

[a] *National Institute of Materials and Chemical Research (MINC), Tsukuba, Ibaraki 305, Japan*

[b] *Research Laboratory of Resource Utilization, Tokyo Institute of Technology (TIT), Yokohama 227, Japan*

Abstract

New layered compounds, $A_4Ta_xNb_{6-x}O_{17}$ (A = K or Rb, $x = 2$, 3, 4 and 6), which had two different kinds of interlayer spaces were prepared. It was found that these compounds with intercalated nickel metal particles showed a marked photocatalytic activity for an overall water splitting. The rate of H_2 and O_2 evolution on Ni–$Rb_4Ta_6O_{17}$ was smaller than that on Ni–$Rb_4Nb_6O_{17}$ because $Rb_4Ta_6O_{17}$ had a larger band gap than that of $Rb_4Nb_6O_{17}$. The quantum efficiencies (< 250 nm) for both materials were, however, almost the same. In the case of Ni–$K_4Ta_xNb_{6-x}O_{17}$, the rate of H_2 and O_2 evolution decreased with the increase of Ta substitution though the threshold of UV absorption shifted to longer wavelength, suggesting that the extended absorption to a longer wavelength did not contribute to the photocatalytic water splitting. It was also found that $A_4Ta_xNb_{6-x}O_{17}$ itself without any modification could decompose water, which confirmed that the structure consisting of two different kinds of interlayer spaces is essential for water splitting.

Keywords: Photocatalytic water splitting; Nickel

1. Introduction

It is known that nickel intercalated $A_4Nb_6O_{17}$ (A = K, Rb) shows an excellent photocatalytic activity for the water decomposition with high quantum efficiency (5–10% at 330 nm) [1–3]. $A_4Nb_6O_{17}$ is an ion-exchangeable layered compound having corrugated niobium oxide sheets stacked along the b-axis of an orthorhombic unit cell. A unique structural feature of these compounds is the existence of two different kinds of alternative interlayer spaces (interlayer spaces I and II). However, the chemical properties of these interlayer spaces are very different: e.g., Ni^{2+} ion intercalates only into the interlayer I. A mechanism of the photodecomposition of water on the catalyst has been proposed taking the layered structure into account: the intercalated water is reduced to H_2 in the interlayer I and is oxidized to O_2 in the interlayer II [4]. To further examine the photocatalytic activity and the reaction mechanism of the unique material, we prepared several new layered oxides belonging to the same family with $K_4Nb_6O_{17}$, i.e., $A_4Ta_xNb_{6-x}O_{17}$ (A: K or Rb, $x = 2$, 3, 4 and 6). It was found that the newly prepared compounds show good photocatalytic activities for the water decomposition. The unique specificity of the structure upon photocatalytic water splitting was discussed.

* Corresponding author.

SSDI 0920-5861(95)00224-3

2. Experimental

For the preparation of $K_4Ta_xNb_{6-x}O_{17}$, the stoichiometric mixture of K_2CO_3, Ta_2O_5 and Nb_2O_5 was pressed in the form of a pellet, heated in air at 1573–1773 K for 15 min, and then cooled rapidly. The preparation of $Rb_4Ta_xNb_{6-x}O_{17}$ was more complex as follows: an excess amount of Rb of 5 to 15 mol% than the stoichiometric one was added. A pellet of the mixture of Rb_2CO_3, Ta_2O_5 and Nb_2O_5 was heated at 1175–1523 K for 40 h, and then it was cooled down gradually to 1023 K (cooling rate 15 K/h) and further to room temperature. Their structures were examined by XRD measurements. Before nickel loading, $Rb_4Ta_xNb_{6-x}O_{17}$ was washed by distilled water and recalcined in air at 1173 K for 10 h as mentioned in the previous paper [3]. The procedure for $Rb_4Ta_xNb_{6-x}O_{17}$ preparation was essential to obtain a high catalytic activity. Nickel-intercalated photocatalysts were prepared by an ion-exchange method immersing an aqueous solution of $Ni(NO_3)_2$ for 1 h, and were reduced by H_2 at 773 K for 2 h and oxidized by O_2 at 473 K for 1 h. The photocatalytic reaction was carried out in a closed gas-circulating system with an inner irradiation quartz reactor. A catalyst (1 g) was dispersed in distilled water (350 ml) and the system was degassed completely, then Ar gas was introduced up to 4.6 kPa. The catalyst was suspended by rapid stirring and irradiated using a high-pressure Hg lamp (Riko Kagaku, 400 W). The lamp was covered with a quartz water jacket, and the reaction temperature was kept constant (293 K). The amounts of evolved H_2 and O_2 were analyzed by a gas chromatograph (TCD, molecular sieve 5A) and pressure sensor.

3. Results and discussion

3.1. Characterization of $A_4Ta_xNb_{6-x}O_{17}$

The XRD patterns of various $A_4Ta_xNb_{6-x}O_{17}$ (A = K and Rb, $0 \leq x \leq 6$) were closely resembled each other except $K_4Ta_6O_{17}$. Various preparation methods were tried to synthesize $K_4Ta_6O_{17}$ with layered structure, however, all of them were only mixtures of $KTaO_3$ and Ta_2O_5. Fig. 1 shows SEM photographs of Ni–$Rb_4Ta_6O_{17}$. It shows a mica-like layered struc-

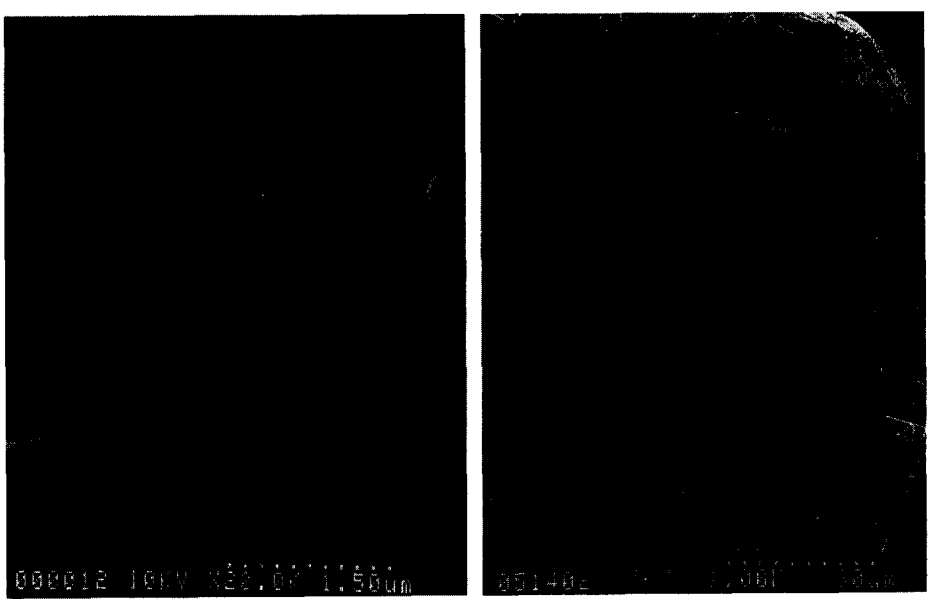

Fig. 1. SEM photographs of Ni(0.1 wt%)–$Rb_4Ta_6O_{17}$.

Table 1
Characteristics of $A_4Ta_xNb_{6-x}O_{17}$ (A = K, Rb; $0 < x < 6$)

x, catalyst	b-axis length (Å) [a]		Threshold of UV absorption (nm)
	Anhydrate	Hydrate	
0, $K_4Nb_6O_{17}$	33.2	37.6	360
2, $K_4Ta_2Nb_4O_{17}$	33.2	39.3	365 (400)
3, $K_4Ta_3Nb_3O_{17}$	34.5	39.3	380 (400)
4, $K_4Ta_4Nb_2O_{17}$	34.5	39.4	410
6, $(K_4Ta_6O_{17})$ [b]	–	–	360
0, $Rb_4Nb_6O_{17}$	33.2	39.1	360
2, $Rb_4Ta_2Nb_4O_{17}$	34.2	39.2	350
3, $Rb_4Ta_3Nb_3O_{17}$	34.5	39.2	345
4, $Rb_4Ta_4Nb_2O_{17}$	34.5	39.4	345
6, $Rb_4Ta_6O_{17}$	34.5	39.4	295
Ta_2O_5			330
Nb_2O_5			370
$KTaO_3$			350
$KNbO_3$			410

[a] Calculated by d(040).
[b] $K_4Ta_6O_{17}$ was a mixture of $KTaO_3$ and Ta_2O_5 etc., which did not have a layered structure.

ture. The values of b-axis length are shown in Table 1. It is known that the interlayer space I of $K_4Nb_6O_{17}$ is hydrated in an atmosphere ($K_4Nb_6O_{17} \cdot 3H_2O$) and b-axis length increases [5]. $A_4Ta_xNb_{6-x}O_{17}$ were also hydrated in a humid atmosphere and b-axis length of them increased by intercalation of H_2O. The b-axis lengths of both hydrated and anhydrated compounds increased with substitution of Ta for Nb.

Diffuse reflectance UV spectra of (a) $K_4Ta_xNb_{6-x}O_{17}$ and (b) $Rb_4Ta_xNb_{6-x}O_{17}$ are shown in Fig. 2. In the case of (b) $Rb_4Ta_xNb_{6-x}O_{17}$, the absorption threshold of UV spectra shifted to shorter wavelength with an increase of Ta substitution for Nb. The threshold of $Rb_4Ta_6O_{17}$ spectrum was 295 nm and band gap was roughly estimated to be 4.1 eV, which was very large value compared with other conventional semiconductor catalysts such as TiO_2 and $SrTiO_3$. On the other hand, the threshold of spectra of (a) $K_4Ta_xNb_{6-x}O_{17}$ shifted to longer wavelength with Ta substitution up to $x = 4$. The absorption threshold of $K_4Ta_4Nb_2O_{17}$ was located in visible region and its color was slightly yellow. When Ta was substituted for all Nb ($x = 6$), the layered structure was not formed and the threshold of UV spectrum shifted to shorter wavelength.

The band gap and potential of the conduction band bottom of a metal oxide semiconductor are influenced by the kinds of metals and the crystal

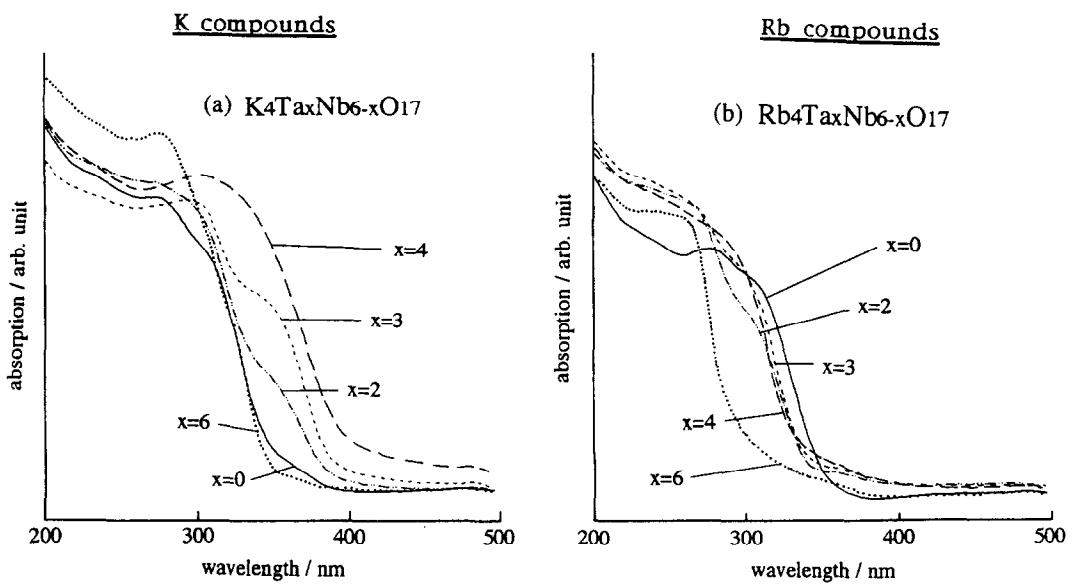

Fig. 2. UV-diffuse reflectance spectra. (a) $K_4Ta_xNb_{6-x}O_{17}$, and (b) $Rb_4Ta_xNb_{6-x}O_{17}$.

structures. The band gaps of tantalum compounds are usually larger than that of niobium compounds, probably because the conduction bands of Ta and Nb compounds originate from 5d orbitals of Ta and 4d orbitals of Nb, respectively, and the potential energy of 5d orbitals is higher than that of 4d orbitals. Actually, the flat band potential of Ta_2O_5 (−0.4 eV NHE, pH 0) is higher than that of Nb_2O_5 (0 eV NHE, pH 0) [6]. Both the valence bands of tantalum oxides mainly and niobium oxides originate from 2p orbitals of oxygen atom. From these results, it is understood that the band gap of the mixed oxide of Ta and Nb increase with Ta substitution for Nb in the case of $Rb_4Ta_xNb_{6-x}O_{17}$. In the case of $K_4Ta_xNb_{6-x}O_{17}$, the shift of UV absorption edge to longer wavelength may be explained by distortion of its crystal structure and/or formation of lattice defects. The distortion of $K_4Ta_xNb_{6-x}O_{17}$ structure is considered to increase with Ta substitution, because the full substitution of Ta for Nb leaded to collapse of the layered structure. A similar kind of red shift of UV absorption edge was reported on $Na_{2-6x}(Ti_{1-x})_6O_{13}$ [7]. At present, it is not clear which band, i.e., the conduction or the valence bond is more affected by the substitution.

3.2. *Photocatalytic decomposition of water over Ni-intercalated $A_4Ta_xNb_{6-x}O_{17}$*

Table 2 shows the photocatalytic activity for water decomposition on Ni-intercalated $A_4Ta_xNb_{6-x}O_{17}$. Water is decomposed into H_2 and O_2 in a stoichiometric ratio on all the photocatalysts and the evolution rates of the gases are constant even after more than 20 h. The rates of H_2 and O_2 evolution over Ni(0.1 wt.%)–$Rb_4Nb_6O_{17}$ were 936 μmol/h (51.9 torr/h) and 451 μmol/h (28.4 torr/h), respectively. To attain the stoichiometric evolution of H_2 and O_2 over Ni–$Rb_4Mb_6O_{17}$, it was necessary to pretreat $Rb_4Nb_6O_{17}$ by washing and calcination before Ni loading to remove excess Rb [3]. In the case of $Rb_4Ta_xNb_{6-x}O_{17}$, such pretreatments were also necessary for the stoichiometric decomposition of water. A typical time course of H_2 and O_2 evolution from distilled water over Ni(0.1 wt.%)–$Rb_4Ta_6O_{17}$ is shown in Fig. 3. After an induction period of less than 1 h, H_2 and O_2 evolved steadily in the stoichiometric ratio. The rate of gas evolution was remarkably enhanced by the pretreatments.

Table 2
Photocatalytic activity over Ni–$A_4Ta_xNb_{6-x}O_{17}$ (A = K, Rb; $0 < x < 6$)

x	Catalyst	Rate of gas evolution (μmol/h)	
		H_2	O_2
0	Ni–$K_4Nb_6O_{17}$	403	197
2	Ni–$K_4Ta_2Nb_4O_{17}$	409	198
3	Ni–$K_4Ta_3Nb_3O_{17}$	233	111
4	Ni–$K_4Ta_4Nb_2O_{17}$	31	12
0	Ni–$Rb_4Nb_6O_{17}$ [a]	936	451
2	Ni–$Rb_4Ta_2Nb_4O17$ [a]	362	179
3	Ni–$Rb_4Ta_3Nb_3O_{17}$ [a]	126	62
4	Ni–$Rb_4Ta_4Nb_2O_{17}$ [a]	101	48
6	Ni–$Rb_4Ta_6O_{17}$ [a]	92	46
6	Ni–$Rb_4Ta_6O_{17}$	11	1
	Ni–Nb_2O_5	1	0
	Ni–$KNbO_3$	1	0
	Ni–KNb_3O_8	1	0
	Ni–Ta_2O_5	4	1
	Ni–$KTaO_3$	6	2

0.1 wt.% nickel was loaded. Catalyst, 1 g; distilled water, 350 ml; high pressure Hg lamp (400 W); inner irradiation cell (quartz).
[a] After activation treatment (washing and recalcination in air at 1173 K for 10 h).

The photocatalytic activity decreased with the increase of Ta atom substitution for Nb atom. The fact that the rate of gas evolution over Ni–$Rb_4Ta_6O_{17}$ was less than that over Ni–$Rb_4Nb_6O_{17}$ was mainly explained by the difference of the band gap energies of the catalysts. The band gap of $Rb_4Ta_6O_{17}$ was estimated at about 4.1 eV by UV diffuse reflectance spectrum. It was much larger than that of $Rb_4Nb_6O_{17}$ (ca. 3.5 eV). The amount of photon absorbed by $Rb_4Ta_6O_{17}$ is much less than that by $Rb_4Nb_6O_{17}$. Table 3 shows the rate of H_2 evolution over Ni–$A_4Ta_xNb_{6-x}O_{17}$ under irradiation with or without Na_2CO_3 solution

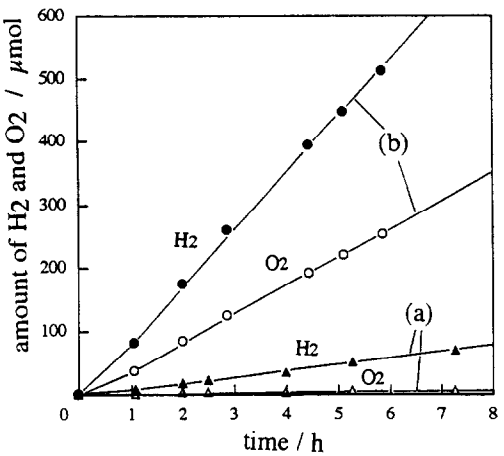

Fig. 3. Time course of H_2 and O_2 evolution from distilled water over Ni(0.1 wt%)–$Rb_4Ta_6O_{17}$. (a) before the activation treatment (H_2: ●, O_2: ○), and (b) after the activation treatment (H_2: ▲, O_2: △). The activation treatment: $Rb_4Ta_6O_{17}$ was washed well by distilled water, and then it was calcined in air at 1173 K for 10 h.

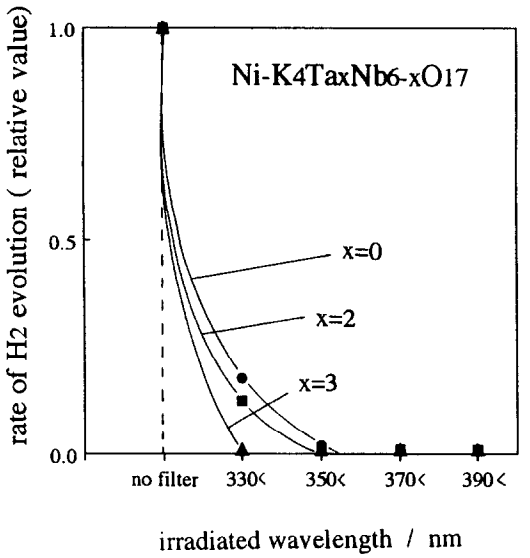

Fig. 4. Dependence of rate of H_2 evolution over Ni(0.1 wt%)–$K_4Ta_xNb_{6-x}O_{17}$ upon the irradiation wavelength. Outer irradiation type quartz reactor and high pressure Hg lamp were used. "330 <" means that the UV light less than 330 nm was cut by the 330 nm cut-off filter. The rate of gas evolution was a relative value (the rate of H_2 evolution without filter was in agreement with 1.0).

filter. The saturated Na_2CO_3 solution absorbs light less than 250 nm. The absorption of light by Na_2CO_3 solution should cause the decrease of H_2 evolution rate attributed to photons less than 250 nm. The decrease of photon flux was constant in each measurement. Comparing the decrease of H_2 evolution rate ($R_b - R_a$ in Table 3) between Ni–$Rb_4Nb_6O_{17}$ and Ni–$Rb_4Ta_6O_{17}$, they were almost the same values and it suggested the efficiencies of water splitting were comparable for both catalysts in this wavelength region.

Table 3
Rate of gas evolution over Ni–$A_4Ta_xNb_{6-x}O_{17}$ under UV irradiation with or without Na_2CO_3 solution filter

Catalyst	H_2 evolution rate (μmol/h)		$R_b - R_a$
	Without solution filter (R_a)	Na_2CO3 solution filter (R_b) [a]	
Ni–$K_4Nb_6O_{17}$	403	393	−10
Ni–$K_4Ta_4Nb_2O_{17}$	31	28	−3
Ni–$Rb_4Nb_6O_{17}$	936	921	−15
Ni–$Rb_4Ta_6O_{17}$	92	75	−17

Catalyst, 1 g; distilled water, 350 ml; high pressure Hg lamp (400 W); inner irradiation type cell.
[a] The lamp was covered with a double water jacket made of quartz. Cooling water was flowed in the inner water jacket. Saturated Na_2CO_3 solution was located in the outer water jacket.

In the case of Ni–$K_4Ta_xNb_{6-x}O_{17}$ ($x = 0$–4), the threshold of spectra shifted to longer wavelength with increase of Ta substitution. The number of absorbed photon by $K_4Ta_4Nb_2O_{17}$ should be larger than that by $K_4Nb_6O_{17}$. A shift of absorption edge to longer wavelength is very favorable for effective utilization of solar energy by photocatalytic water splitting. However, it was found that the rate of gas evolution decreased with the increase of Ta substitution. From Table 3, the decrease of H_2 evolution caused by Na_2CO_3 filter on Ni–$K_4Ta_4Nb_2O_{17}$ was smaller than that over Ni–$K_4Nb_6O_{17}$. Therefore, the quantum efficiency of Ni–$K_4Ta_4Nb_2O_{17}$ was smaller than Ni–$K_4Nb_6O_{17}$ less than 250 nm. Fig. 4 shows the dependence of the rate of H_2 evolution on Ni(0.1 wt.%)–$K_4Ta_xNb_{6-x}O_{17}$ upon the irradi-

ation wavelength. The outer irradiation type quartz reactor equipped with high-pressure Hg lamp (500 W) was used. The indication of "330 <" means that the UV light of wavelength less than 330 nm was cut by the 330 nm cut-off filter. It was found that the threshold of the effective wavelength for the photocatalytic water splitting on Ni–$K_4Ta_xNb_{6-x}O_{17}$, shifted to shorter wavelength with the increase of Ta substitution. For example, the active wavelength of Ni–$K_4Ta_3Nb_3O_{17}$ for water splitting was less than 330 nm, and its absorption edge was extended to 410 nm but not active at all. The extended absorption to longer wavelength might be attributable to localized level derived from lattice defect.

Besides the difference of the band gap, we have to consider several other factors which affect the photocatalytic activity, because the rate of gas evolution on Ni–$Rb_4Nb_6O_{17}$ was twice larger than that on Ni–$K_4Nb_6O_{17}$. For example, the presence of recombination sites of electrons and holes, the width of interlayer spaces and the dispersion of nickel metal in the interlayer I might also affect the photocatalytic activity. It is speculated that the defect levels of $K_4Ta_xNb_{6-x}O_{17}$ might act as recombination sites.

3.3. *Photocatalytic decomposition of water on $A_4Ta_xNb_{6-x}O_{17}$ without any modification*

What we want to clarify in this study is the relationship between the structure which have two kinds of interlayers and the activity of photocatalytic decomposition of water. The series of the layered compounds mentioned above could decompose water with loading of nickel metal as shown in Table 2. The uniqueness of the structure of $A_4Nb_6O_{17}$ upon the water splitting was already demonstrated [8]. The other compounds such as Ni–Nb_2O_5, Ni–$KNbO_3$ and Ni–KNb_3O_8 could not decompose water. On the other hand, the results of Table 2 do not show the clear specificity of the structure of $A_4Ta_xNb_{6-x}O_{17}$. Although Ni(0.1 wt.%)–Ta_2O_5 [9] and Ni(0.1 wt.%)–$KTaO_3$ had the activity of water splitting, the rates of gas evolution were much smaller than that of Ni(0.1 wt.%)–$Rb_4Ta_6O_{17}$.

The photocatalytic decomposition of water on some of those catalysts without any loaded metals was carried out in order to clarify the specificity of the structure of $A_4Ta_xNb_{6-x}O_{17}$. From our previous work all semiconductors except for ZrO_2 needed loaded metals, such as Pt, Rh, Ni, RuO_2, etc., for the photocatalytic decomposition of water. The loaded metals were regarded to work for the acceleration of charge separation, the formation of reaction sites, the decrease of overpotential and so on [10,11]. ZrO_2 can decompose water stoichiometrically without any loaded metals. The characteristics of ZrO_2 is believed to be associated with its highly negative flat-band potential (-1.0 eV NHE, pH 0) and very wide band gap (5.0 eV) [12]. It is also reported that $K_4Nb_6O_{17}$ without any loaded metals could evolve H_2 and O_2 simultaneously though the ratio of H_2 and O_2 evolution was not exactly stoichiometric [1]. In this study, it was found that $K_4Nb_6O_{17}$ could decompose water stoichiometrically by the following pretreatment: i.e., high temperature reduction by H_2 at 973 K for 6 h and re-oxidation by O_2 at 473 K for 1 h (R973-O473) as shown in Table 4. After the pretreatment, $Rb_4Ta_6O_{17}$ as well as $Rb_4Nb_6O_{17}$ had the activity for the stoichiometric water splitting. However, Ta_2O_5 and $KTaO_3$ could not decompose water at all. These results clearly show that the structure of $A_4Ta_xNb_{6-x}O_{17}$ is specifically active for the water photo-splitting reaction. We proposed the following reaction mechanism over $K_4Nb_6O_{17}$ previously: the charge separation of e^- and h^+ in the niobium oxide sheet occurred because chemical and physical properties of two interlayer spaces were very different.

Therefore H_2 and O_2 evolved in different interlayer spaces, respectively. The charge separation and the different reaction sites for H_2 and O_2 evolution are very important factors for water splitting, and structure of $A_4Ta_xNb_{6-x}O_{17}$

Table 4
Photodecomposition of water over several semiconductor catalysts without metal modification

Semiconductor	Pretreatment [a]	Rate of gas evolution (μmol/h)		
		H_2	O_2	H_2/O_2
$K_4Nb_6O_{17}$	Untreated	14	2	7.0
	R573-O473	22	8	2.8
	R773-O473	26	10	2.6
	R973-O473	57	28	2.0
	R973	45	14	3.2
$Rb_4Nb_6O_{17}$	R973-O473	98	45	2.2
$Rb_4Ta_3Nb_3O_{17}$	R973-O473	46	22	2.1
$Rb_4Ta_6O_{17}$	R973-O473	23	11	2.1
KNb_3O_8	R973-O473	1	0	–
Nb_2O_5	R973-O473	0	0	–
Ta_2O_5	R973-O473	2	0	–
TiO_2	R973-O473	2	0	–
$SrTiO_3$	R973-O473	1	0	–

Catalyst, 1 g; distilled water, 350 ml; high pressure Hg lamp (400 W); inner irradiation cell (quartz).
[a] R973: H_2 reduction at 973 K for 6 h. R973-O473: O_2 oxidation at 473 K for 1 h after R973.

intrinsically have these functions especially. Thus, the structure of $A_4Ta_xNb_{6-x}O_{17}$ was especially suitable for the water splitting.

The reason why the pretreatment can promote the activity of the water splitting is not clear at present. It may be speculated that the photo-adsorption of O_2 and the formation of peroxide on the catalyst surface is suppressed by the treatment.

4. Conclusion

In this study, the photocatalytic behavior of $A_4Ta_xNb_{6-x}O_{17}$ catalysts was examined. Main results are summarized as follows:

(1) New layered compounds, $A_4Ta_xNb_{6-x}O_{17}$ (A = K or Rb, $x = 2$, 3 and 4) and $Rb_4Ta_6O_{17}$, which had two different kinds of interlayer spaces were prepared. These compounds with intercalated nickel-metal loading showed good photocatalytic activity for the water splitting.

(2) Such as ZrO_2, $A_4Ta_xNb_{6-x}O_{17}$ without any loaded metals could also decompose water stoichiometrically after the following pretreatment: H_2 reduction at 973 K for 6 h and O_2 re-oxidation at 473 K for 1 h. It was suggested that the structure which had two different kinds of interlayer spaces was very suitable for water splitting essentially.

(3) The rate of gas evolution over Ni–$Rb_4Ta_6O_{17}$ was smaller than that over Ni–$Rb_4Nb_6O_{17}$. This is mainly because $Rb_4Ta_6O_{17}$ has a larger band gap than $Rb_4Nb_6O_{17}$. Both quantum efficiencies (< 250 nm) were almost the same.

(4) In the case of $K_4Ta_xNb_{6-x}O_{17}$ ($0 \leq x \leq 4$), the threshold of UV absorption spectra shifted to longer wavelength with increase of Ta substitution. This shift may be attributed to by the distortion of the structure or the defects of the lattice, and the extended absorption to longer wavelength did not contribute to the water splitting at all.

(5) The rate of gas evolution on Ni–$A_4Ta_xNb_{6-x}O_{17}$ decreased with increase of Ta substitution. Several factors as well as the difference of band gap might affect the photocatalytic activity. Especially, the lattice defect in the $K_4Ta_xNb_{6-x}O_{17}$ might act as recombination site. Therefore, the quantum efficiency of Ni–$K_4Ta_4Nb_2O_{17}$ was smaller than Ni–$K_4Nb_6O_{17}$.

Acknowledgements

The authors gratefully thank Dr. J.N. Kondo of TIT for her helpful discussion.

References

[1] A. Kudo, A. Tanaka, K. Domen, K. Maruya, K. Aika and T. Onishi, J. Catal., 111 (1988) 67.
[2] K. Sayama, A. Tanaka, K. Domen, K. Maruya and T. Onishi, Catal. Lett., 4 (1990) 217.
[3] K. Sayama, A. Tanaka, K. Domen, K. Maruya and T. Onishi, J. Catal., 124 (1990) 541.
[4] A. Kudo, K. Sayama, A. Tanaka, K. Asakura, K. Domen, K. Maruya and T. Onishi, J. Catal., 120 (1989) 337.

[5] K. Nassau, J.W. Shiever and J.L. Bernstein, J. Electrochem. Soc., 116 (1969) 348.
[6] H. Maruska and A. Ghosh, Solar Energy, 20 (1978) 443.
[7] Y. Inoue, T. Kubokawa and K. Sato, J. Phys. Chem., 95 (1991) 4059.
[8] K. Domen, A. Kudo, A. Shinozaki, A. Tanaka, K. Maruya and T. Onishi, J. Chem. Soc., Chem. Commun., (1986) 356.
[9] K. Sayama and H. Arakawa, J. Photochem. Photobiol. A: Chem., 77 (1994) 243.
[10] T. Sakata, K. Hashimoto and T. Kawai, J. Phys. Chem., 88 (1984) 5214.
[11] M. A. Grätzel, Energy Resources Through Photochemistry and Catalysis, Academic Press, New York, 1983.
[12] K. Sayama and H. Arakawa, J. Phys. Chem., 97 (1993) 531.